

Received January 24, 2020, accepted February 20, 2020, date of publication February 28, 2020, date of current version March 11, 2020.

Digital Object Identifier 10.1109/ACCESS.2020.2977173

# Modelling Coverage Failures Caused by Mobile Obstacles for the Selection of Faultless Visual Nodes in Wireless Sensor Networks

THIAGO C. JESUS<sup>1,2</sup>, DANIEL G. COSTA<sup>1</sup>, (Senior Member, IEEE), PAULO PORTUGAL<sup>2</sup>, FRANCISCO VASQUES<sup>2</sup>, AND ANA AGUIAR<sup>3</sup>

<sup>1</sup>Department of Technology, State University of Feira de Santana, Feira de Santana 44036-900, Brazil

<sup>2</sup>INEGI/INESC-TEC, Faculty of Engineering, University of Porto, 4200-465 Porto, Portugal

<sup>3</sup>Instituto de Telecomunicações (IT), University of Porto, 4200-465 Porto, Portugal

Corresponding author: Daniel G. Costa (danielgcosta@uefs.br)

This work was a result of the project Operation NORTE-08-5369-FSE-000003 supported by Norte Portugal Regional Operational Programme (NORTE 2020), under the PORTUGAL 2020 Partnership Agreement, through the European Social Fund (ESF). Additionally, this work was also partially funded by the Brazilian CNPq Agency (grant 204691/2018-4) and by the projects MobiWise (SAICTPAC/0011/2015, POCI-01-0145-FEDER-016426) and S2MovingCity (CMUP-ERI/TIC/0010/2014), as well as the IT (UID/EEA/50008/2019) Research Units, funded by the applicable financial framework: Fundo Europeu de Desenvolvimento Regional (FEDER), Programa Operacional Competitividade e Internacionalização (POCI), FCT/MCTES (Portuguese Foundation for Science and Technology).

**ABSTRACT** Wireless sensor networks comprising nodes equipped with cameras have become common in many scenarios, providing valuable visual data for some relevant services such as localization, tracking, patterns identification and emergencies detection. In this context, algorithms and optimization approaches have been designed to perform different types of quality assessment or performance enhancement tasks, addressing challenging issues such as networking, compression, availability, reliability, security, energy efficiency and virtually any subject related to the operational challenges of those networks. However, the dynamics of coverage failures have not been properly modelled in visual sensor networks, resulting in unrealistic perceptions when optimizing or assessing quality in most visual sensing scenarios. Particularly, the Field of View of visual sensors will be affected by occlusion caused by obstacles in the monitored field, which may turn such sensors inadequate for the expected monitoring services of the considered network. Therefore, this article proposes a mathematical model to assess occlusion caused by mobile obstacles such as vehicles on a road or forklifts in an industrial plant, aiming at the selection of the visual sensor nodes that will not have their coverage significantly restricted by those obstacles. Doing so, the proposed model can be exploited by any optimization or quality assessment approach in wireless visual sensor networks, providing a preprocessing method when selecting visual nodes.

**INDEX TERMS** Wireless sensor networks, visual sensing, sensors selection, coverage failures, mathematical modelling.

## I. INTRODUCTION

The development of low-cost highly programmable hardware platforms and Systems on a Chip (SoC) devices have deeply transformed the way sensing and monitoring applications have been created and deployed, opening new possibilities for Wireless Sensor Networks (WSN) [1], [2]. In this evolving scenario, the constant adoption of cameras to gather visual data has been a breakthrough in many applications, not only impacting on the development of Wireless Visual Sensor

Networks (WVSN) themselves, but also fostering the maturation of the Internet of Things (IoT) landscape [3], [4]. The resulting scenario of sensors-based visual monitoring has been permeated by applications in different contexts, benefiting Smart Cities [5], Industry 4.0 [6], IoT-based Agriculture [7] and many others distributed sensing initiatives [8].

Wireless visual sensor networks have experienced many complex challenges as sensing and communication technologies evolve and new sensing demands arise [9], [10]. In this sense, the resource-demanding nature of visual data processing and transmissions, as well as the real-time delivery requirements of some applications, have stimulated

The associate editor coordinating the review of this manuscript and approving it for publication was Shunfeng Cheng.

researches on different aspects of the wireless visual sensor networks operation cycle, aiming at different types of optimizations. For example, some works have proposed mechanisms to optimize the way routing paths are created to deliver visual data, as in [11], [12]. In a different perspective, dependability and availability of wireless visual sensor networks have been optimized in the context of visual sensing, as performed in [13], [14]. Moreover, visual coverage optimizations have also been proposed, trying to improve the attainable viewed areas and targets by visual sensors, as in [15], [16]. Finally, energy consumption associated to visual data quality is also susceptible to optimizations, as in [17]. In fact, all those works have proposed some kind of optimization to improve the quality of some aspects of visual sensor networks, bringing promising results.

Although optimization approaches have been proposed to handle the multiple challenges of WWSN, most works have not been concerned with coverage failures [18], [19]. Actually, in a different way of (scalar) sensor networks, the use of cameras has some relevant particularities that should be properly accounted when performing most optimization approaches. In order to illustrate this matter, a sensor network composed of a dozen of cameras may be optimized to reduce energy consumption resulted from transmissions of visual data from source nodes, for example performing efficient compression of the original raw visual data. However, if regular cameras are employed on an outdoor scenario, they may become useless during the night and any employed optimization approach might not accomplish the expected results. In a different scenario but with similar outcome, visual sensors may be occluded by obstacles, which will reduce their effectively viewed areas [20]. Therefore, any performed optimization or quality assessment approach in wireless visual sensor networks should only consider visual sensors that are not under any coverage failure, at the risk of having their results compromised.

Regarding this perspective over visual sensing, the coverage failures assume a relevant role when perceiving a WWSN and thus those failures should be properly known and modelled [21]. Among the most common coverage failures, occlusion may be particularly prejudicial for many monitoring scenarios, severely impacting the functions of the visual sensors for the considered network. Actually, this is indeed the key question when performing any kind of optimization in WWSN: which are the visual sensors that can be selected as contributing to the monitoring functions of the network? But the answer to this question may be hard to find, also changing during a network lifetime.

This article proposes the modelling of occlusion in order to select visual sensors that are not under a coverage failure, determining a minimum accepted percentage of visual coverage ( $C_{min}$ ) as a defining parameter. The obstacles are modelled as being mobile 2D rectangles, which are reasonable simplifications of real objects, potentially assuming any possible position and orientation along the time. Then, the Field of View (FoV) triangle defined by each visual sensor

is processed against a set of mobile obstacles (rectangles), resulting in convex or concave polygons for each visual sensor. The computation of those Occluded FoV (OFoV) requires a series of Geometry and Trigonometry rules and a set of heuristics that had to be proposed to handle with this complex mathematical problem.

The proposed approach, which aims to geometrically compute the resulted FoV of the visual sensors that are being occluded by mobile obstacles, could substitute costly computer vision algorithms, processing the entire network in a central unit. Exploiting this model, a preprocessing mechanism is then proposed to take a number of visual sensors and mobile obstacles as input, computing the resulting set of active visual sensors. Such computed set can be processed as an input to any existing optimization or quality assessment approach. This innovative methodology might be further extended to include any other type of coverage failure, since this is a broader concept to be exploited, significantly contributing to the development of the wireless visual sensor networks research area. To the best of our knowledge, this coverage modelling problem and the methodology for faultless visual sensors section have not been addressed before.

The remainder of this article is organized as follows. Section II discusses some important related works. Section III defines the fundamentals of the considered mobile obstacles. The proposed mathematical model for visual occlusion computation is described in Section IV. The methodology for selection of faultless visual sensors is presented in Section V. Section VI brings initial numerical results. A discussion about the use of visual sensors selection as a tool to support other research works is conducted in Section VII, followed by conclusions and references.

## II. RELATED WORKS

Wireless visual sensor networks have been advocated as an important piece of the Internet of Things revolution, providing visual data as images and videos for an uncountable number of applications. However, it has not been straightforward in the sense that many complexities are related to the adoption of visual sensing in IoT scenarios. As a result, many research works have proposed different approaches to better support such networks, influencing this article in different ways.

Sensor nodes equipped with one or more cameras are able to gather visual data from the environment and to process and transmit such data to any application at the sink side. Since this is the basic expected function from visual sensor nodes, the way they will achieve the coverage objectives of the applications is of paramount importance. Therefore, WWSN research works have been concerned with coverage quality assessment and enhancement, in different perspectives.

The primary objective of visual sensors is to view part of the monitored field and sometimes the quality of the network will be a function of this characteristic. But such “viewing” can be performed in different ways and with different objectives. In fact, coverage assessment as an indication of “quality” has been investigated in the last years by many

research works, achieving different promising results. The work in [22] proposed a distributed mechanism to optimize coverage, associating the coverage quality with the energy efficiency of the network. The work in [23] proposed a new methodology to assess quality when performing barrier coverage, also defining an optimization mechanism to increase coverage in such scenario. In [24], a metric referred as Quality of Viewing (QoV) was proposed to extend the traditional perception of Quality of Service (QoS) when assessing the performance of applications based on visual sensors. The QoV is expected to be employed to measure the quality of retrieved data for the monitoring requirements of the applications and thus it depends on the particularities of each considered scenario. Coverage assessment and improvement were also performed in [25], which optimized the orientation of cameras for indoor monitoring. Metrics for coverage of targets and areas have also been proposed in the last years, being discussed and compared in some works [15], [26].

Other relevant metric for visual sensing is “availability”, since it allows the perception of “coverage quality” in a more comprehensive way. In such case, the visual coverage would be one component of a wider concept of quality, which would also typically comprise hardware and communication failures as additional parameters. Actually, the processing of visual sensing availability has been investigated in recent years, with some works focusing on different aspects of it. In [27], visual sensing quality was computed as a function of visual sensing redundancy, since it can be exploited when failures occur and faulty nodes have to be replaced. In [16], availability can be measured as a maximization of simultaneous redundant coverage over targets. Such maximization can then be exploited to potentially achieve higher redundancy and increased coverage perspectives over multiple targets. Finally, a robust methodology to integrate different types of hardware and communication failures was proposed in [14], but in that work visual sensors are always considered as active and fully functional when concerning coverage failures, which may be unrealistic in many scenarios.

The visual coverage has also been exploited as a parameter to improve the network quality in other aspects, achieving global results. The work in [28] proposed the exploitation of the overlapping between sensors’ FoV when selecting clustering for communication, potentially reducing energy consumption when redundant nodes are selected. In [13], the way targets (objects) are viewed by visual sensors directly impact the “priority” of visual sensors when transmitting data packets, optimizing the way a network operates.

Concerning mathematical modelling of coverage issues, the work in [29] proposed a model to compute occlusion caused by simplified static obstacles, which were modeled as 2D walls (lines). Actually, that work was focused on FoV overlapping and the maximization of the number of redundant nodes, aimed at enhanced availability. Nevertheless, the work in [29] brought some initial contributions when computing occluded FoV, even under a different objective, influencing our proposed approach.

The state-of-the-art in this subject has then considered visual sensing coverage in different ways, but we could highlight some research trends that influenced our work: coverage **assessment**, coverage **enhancement** and coverage **as quality**. In this context, the proposed approach considers “coverage as quality”, since it is a component for availability processing in wireless visual sensor networks, but employed techniques and methods for coverage assessment and enhancement also contributed to the proposed approach. Table 1 summarizes the reviewed works in this area.

Finally, after defining the scope of problems to be addressed by this work and all related subjects, the literature concerning the particular issue of visual sensing occlusion was surveyed. Actually, some works handled this problem in different ways, giving some clues about the modelling of occlusions. In [31], authors considered occlusion caused by obstacles as a fundamental element when deploying sensor nodes. In that work, an algorithm was proposed to deploy the minimum number of visual sensors, at optimized positions, that can cover the highest number of targets. In [32], occlusion was treated as a coverage problem for a network of Unmanned Aerial Vehicles (UAV). Once again, occlusion was modelled as a parameter for coverage optimization, guiding positioning and movement of the UAV nodes. The work in [29], as discussed before, addressed visual occlusion mathematically, opening possibilities for analyses and estimation of visual coverage by sensor nodes. Some of the formulations in that work are used as reference for some of the proposals in this article.

In fact, occlusion has been a relevant issue for computer vision applications [33], [34], and more recently for visual sensing as well, but under different perspectives. Nevertheless, the proper mathematical modelling of this problem for the selection of visual sensors in WSN had not been addressed before, fostering the development of this work.

### III. MOBILE OBSTACLES

The selection of faultless visual sensor nodes is centered on the identification and processing of a set of mobile obstacles and their impact on the coverage of the considered sensors. Hence, the proposed approach was initially concerned with the proper modelling of the obstacles, with the other elements of this problem (visual nodes, dynamic occlusion and sensors selection) being modelled on a second moment.

Actually, there are different ways to geometrically model obstacles, with different levels of complexity. However, when modelling large WWSN and multiple mobile objects, the perception of the obstacles may be simplified to a line, a square or a circle, using the original dimensions of the obstacles as reference. Such simplifications may allow the processing of visual occlusion as a simpler problem of Geometry, with lower computational complexity and approximated results.

In order to achieve a practical and yet effective mathematical model for the defined problem scope, mobile obstacles will be modeled as rectangles, assuming that a WWSN may

TABLE 1. Coverage research in wireless visual sensor networks.

Work	Assessment	Enhancement	as Quality	Description
Duran-Faundez et al. [13]	-	-	X	A prioritization approach is defined based on visual sensing coverage, setting higher priorities to nodes that can view most relevant parts of the targets
Rangel et al. [16]	-	X	-	Evolutionary algorithms are defined to compute optimized configurations for rotatable visual sensors, aiming at the maximization of redundant coverage
Shahrokhzadeh and Dehghan [22]	-	X	-	Visual sensor nodes are switched off or adjusted to enhance the network visual coverage, exploiting a proposed distributed game theoretic approach
Cheng and Tsai [23]	X	X	-	A coverage metric and optimization algorithms are proposed for barrier coverage, considering visual sensors with and without adjustment capabilities
Costa et al. [24]	X	-	X	A novel metric is proposed to assess the overall quality of visual sensor networks, defining a Quality of Experience (QoE) perception of the applications
Konda et al. [25]	-	X	-	Adjustable cameras are reconfigured to enhance visual sensing coverage, defining the most appropriate camera positions and settings for the nodes
Costa et al. [27]	-	-	X	Redundancy is defined and modelled as a percentage of visual sensing overlapping, allowing the “replacement” of faulty nodes by redundant nodes
Alaei and Barcelo-Ordinas [28]	-	-	X	Visual sensing is exploited to guide the operation of the network, particularly considering visual overlapping
Costa et al. [29]	-	X	X	The occlusion caused by walls are modelled, supporting the identification of redundant visual nodes for enhanced resistance to failures
Costa and Duran-Faundez [30]	X	-	-	A new coverage metric is defined to compute the viewed perimeter of big targets modelled as circles

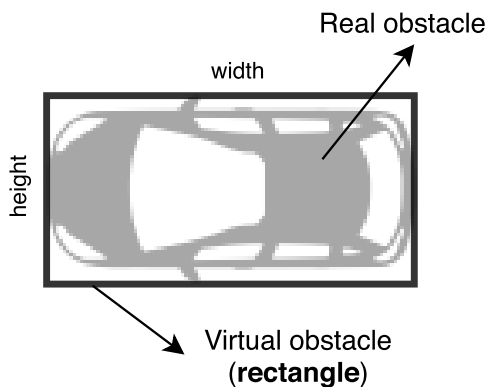


FIGURE 1. The abstraction of mobile obstacles as rectangles.

view  $O$  obstacles with different dimensions. The use of rectangles allows a reasonable simplification of objects, while keeping the intersection of obstacles and FoV's triangles more tractable, although future works may consider other geometric forms as reference.

For any considered obstacle, which may be any moving object (e.g. a car, a truck, a forklift, a tractor), an imaginary rectangle  $o$ , for  $0 < o \leq O$ , will be considered “circumscribing” the obstacle. This modelled rectangle, with width  $w(o)$  and height  $h(o)$ , will represent a virtual and mathematically defined instance of the real obstacle. Fig. 1 presents the generic idea of modelling obstacles as rectangles, which are considered as being perceived from a top-view perspective.

Since obstacles are considered as being mobile, a reasonable simulation mechanism would take real measures from real obstacles, processing such information to better define them. For that, the real obstacles are expected to be equipped with a GPS device, providing real-time data

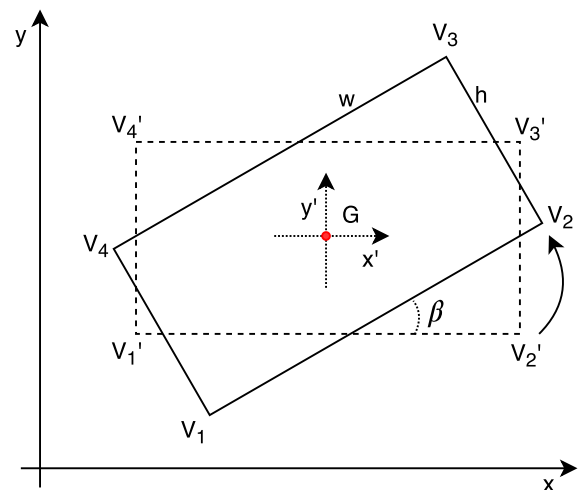


FIGURE 2. The defined mathematical model for the mobile obstacles.

about their location; latitude and longitude data may then be mapped to the position  $(Gx(o), Gy(o))$ , the centroid of the rectangle. Moreover, obstacles may also be equipped with a Gyroscope, providing information about their orientations. Actually, as the obstacles are modelled as rectangles, the Gyroscope will provide the orientation based on the centroid point  $(Gx(o), Gy(o))$ , referred as  $\beta(o)$ .

Fig. 2 depicts the proposed modelling of a mobile obstacle, presenting its centroid, its orientation and the four vertices of the defined rectangle.

With this information, the vertices' coordinates of the obstacle  $o$ ,  $(Vix(o), Viy(o))$ ,  $i = 1, \dots, 4$ , can be computed. For this purpose, an auxiliary coordinate system  $(x', y')$  is defined with its origin at point  $G$ . In  $(x', y')$  it is easy to determine the coordinates  $V'_i(o)$  according to Eq. 1. The next step is to rotate

the obstacle in  $\beta$  degrees to establish its correct orientation. Finally, the auxiliary coordinate system is translated to the original system, obtaining the real  $V_i$  coordinates. Eq. 2 and Eq. 3 present the translation and rotation matrices, respectively. The coordinates  $V_{i(o)}$  are defined by the multiplication of the matrices in the specified order, according to Eq. 4.

$$\begin{aligned} V1'x &= -w/2, & V1'y &= -h/2 \\ V2'x &= w/2, & V2'y &= -h/2 \\ V3'x &= w/2, & V3'y &= h/2 \\ V4'x &= -w/2, & V4'y &= h/2 \end{aligned} \quad (1)$$

$$T(Gx, Gy) = \begin{bmatrix} 1 & 0 & Gx \\ 0 & 1 & Gy \\ 0 & 0 & 1 \end{bmatrix} \quad (2)$$

$$R(\beta) = \begin{bmatrix} \cos(\beta) & -\sin(\beta) & 0 \\ \sin(\beta) & \cos(\beta) & 0 \\ 0 & 0 & 1 \end{bmatrix} \quad (3)$$

$$\begin{bmatrix} Vix \\ Viy \\ 1 \end{bmatrix} = T(Gx, Gy) \cdot R(\beta) \cdot \begin{bmatrix} Vi'x \\ Vi'y \\ 1 \end{bmatrix} \quad (4)$$

The computed vertices of the rectangles are necessary to define the line equations of the obstacles. Actually, an rectangle is composed of four sides and each of those sides can be modelled by a line equation, easing the computation of occlusions exploiting Geometry rules. For any  $(Ox1_{(o)}, Oy1_{(o)})$  and  $(Ox2_{(o)}, Oy2_{(o)})$  points taken from the list of vertices of a obstacle's rectangle, for vertices belonging to the same side of the rectangle ( $V1V2, V2V3, V3V4$  and  $V4V1$ ), Eq. 5 will define each line equation of the obstacle  $o$ , for every valid pair of considered vertices.

$$\overline{O_1O_2} : y - Oy1_{(o)} = \left( \frac{Oy2_{(o)} - Oy1_{(o)}}{Ox2_{(o)} - Ox1_{(o)}} \right) \cdot (x - Ox1_{(o)}) \quad (5)$$

With the definition of the mobile obstacles as rectangles composed of four lines, which are re-computed when obstacles move or rotate, their impact on visual coverage can be mathematically assessed with reasonable complexity, as defined in next section.

## IV. PROPOSED COVERAGE AND OCCLUSION MODEL

### A. VISUAL SENSORS

For the computation of visual occlusion, which is required when selecting faulty nodes, the visual sensors also need to be mathematically processed as virtual nodes. In short, a visual sensor is considered as any sensor device equipped with a camera, being able to gather visual data from the environment. Actually, there are many options when attaching a camera to a sensor, with different configurations [2], and such options can be equally modelled for optimization purposes. Nevertheless, for simplification reasons when performing simulations, we assume a standard configuration to create a reference model, which can be extended in future when necessary.

Every visual sensor node  $s$ , for an initial set of  $S$  visual sensors, will be positioned at the  $(Ax_{(s)}, Ay_{(s)})$  coordinates, assuming that two different sensors can not be deployed at the exact same location. All visual sensors are defined as being static (the initial position is not altered during the considered operation time of the WWSN) and the employed cameras are not rotatable. This is, in fact, a very realistic configuration for visual sensors in many monitoring scenarios, but the proposed model could be easily adapted to support dynamic configurations of the visual sensors with no prejudice to the selection of faultless sensor nodes.

For a 2D model, assuming a top-view perspective of the entire network, each visual sensor will define a Field of View (FoV) according to its viewing angle  $\theta_{(s)}$ , its sensing radius  $r_{(s)}$  and its orientation  $\alpha_{(s)}$ . Actually, there are different approaches on the literature when modelling the sensors' FoV, with different levels of simplification of the Depth of Field (DoF) of the cameras for enhanced mathematical efficiency [15], [26]. In this article, we assume a reasonable perception of the FoV, which is modelled as an isosceles triangle: the vertex  $A$  is the sensors' position while the other vertices can be computed by Trigonometry exploiting the other defined configurations for the visual sensors ( $\theta_{(s)}, r_{(s)}$  and  $\alpha_{(s)}$ ), as expressed in Eq. 6.

$$\begin{aligned} Bx_{(s)} &= Ax_{(s)} + r_{(s)} \cdot \cos(\alpha_{(s)}) \\ By_{(s)} &= Ay_{(s)} + r_{(s)} \cdot \sin(\alpha_{(s)}) \\ Cx_{(s)} &= Ax_{(s)} + r_{(s)} \cdot \cos((\alpha_{(s)} + \theta_{(s)}) \bmod 2\pi) \\ Cy_{(s)} &= Ay_{(s)} + r_{(s)} \cdot \sin((\alpha_{(s)} + \theta_{(s)}) \bmod 2\pi) \end{aligned} \quad (6)$$

Since the area covered by a visual sensor is modelled as an isosceles triangle, the area of any FoV can be computed as expressed in Eq. 7.

$$FoV_{(s)} = \frac{r_{(s)}^2 \cdot \sin(\theta_{(s)})}{2} \quad (7)$$

In the same way of the mobile obstacles, the FoV of the visual sensors can be processed as a group of line equations. For simplicity, each of the three lines that define a FoV's triangle can also be modelled following a specific formulation, as presented in Eq. 8.

$$\begin{aligned} \overline{A_{(s)}B_{(s)}} : y - Ay_{(s)} &= (x - Ax_{(s)}) \cdot \tan(\alpha_{(s)}) \\ \overline{A_{(s)}C_{(s)}} : y - Ay_{(s)} &= (x - Ax_{(s)}) \cdot \tan((\alpha_{(s)} \\ &\quad + \theta_{(s)}) \bmod 2\pi) \\ \overline{B_{(s)}C_{(s)}} : y - By_{(s)} &= \left( \frac{Cy_{(s)} - By_{(s)}}{Cx_{(s)} - Bx_{(s)}} \right) (x - Bx_{(s)}) \end{aligned} \quad (8)$$

Having the line equations of both mobile obstacles and visual sensors, the "interactions" between those elements can be computed and estimated, for any configuration of WWSN. Fig. 3 depicts some of the situations that may happen when visual sensors are occluded by mobile obstacles, presenting all related parameters.

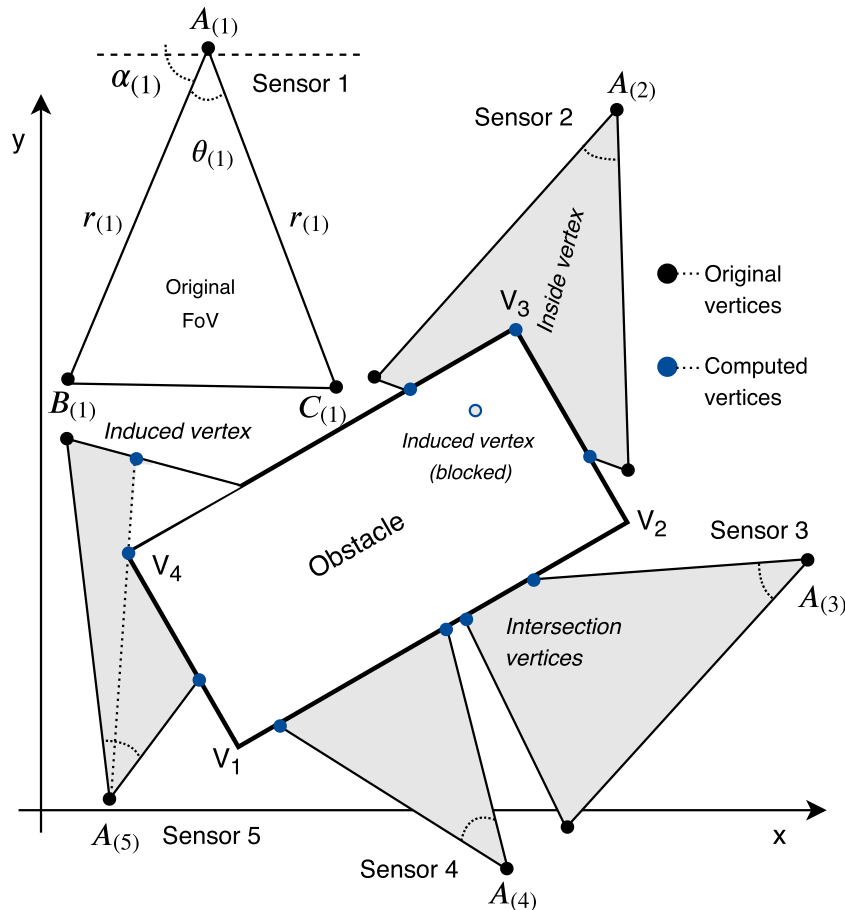


**FIGURE 3.** Different possibilities when visual sensors are being occluded. The shaded areas are the resulted FoV after occlusion (OFoV).

**B. COMPUTING VISUAL OCCLUSION**

The modelling of the visual sensors’ FoV and the obstacles’ rectangles are required to compute the estimated visual occlusion in each of the considered sensors. In fact, any obstacle may interfere in the expected viewed area, reducing the Field of View of the visual sensors. But the actual impact of the obstacles will vary according to the configurations of the visual sensors and the positions and dimensions of the obstacles. In this sense, it is defined the concept of Occluded FoV (OFoV), which is a visual coverage area derived from an original FoV. The OFoV will be modelled as a concave or a convex polygon with an area smaller than the area of the corresponding original FoV triangle. Hence, the computed area of each OFoV will be exploited to identify if a certain visual sensor is under a coverage failure.

Visual occlusion will be computed through the definition of a set of *occlusion vertices*, which are mostly resulted from the intersection of the obstacles’ lines with the visual sensors’ lines. Actually, two lines may not intersect (parallel lines), may intersect in one point (which may be over a FoV’s line or not, in the case the lines extensions meet) or in infinite points (when the lines are coincident). Whatever the case, we can expect that a FoV will be occluded for different

configurations of the obstacles, which may intersect zero or more lines of any FoV, as depicted in Fig. 3.

The OFoV of the visual sensors will be created by the influence of one or more obstacles and thus they may be concave or convex polygons composed of three or more vertices, resulting in  $OFoV(s) < FoV(s)$ . Although an OFoV may be affected by any number of obstacles, they are expected to be processed individually, line by line: the final OFoV is valid when all obstacles that may affect a sensor are considered.

Then, the computation of a set  $L$  of occlusion vertices will involve an original FoV or an OFoV that is not fully processed yet, which will be considered sequentially against unprocessed lines of obstacles. This process is repeated iteratively, until all obstacles’ lines are considered. For that, 6 processing steps were defined, which may or may not achieve a new set of occlusion vertices at the end of each iteration. Therefore, for iteration  $i$ , the set of vertices  $L(i - 1)$  will be considered through 6 processing steps until a new set  $L(i)$  is computed, which is the final OFoV of sensor  $s$  if  $i$  is the last processed iteration. Moreover, for iteration  $i = 1$  (the first iteration), the vertices in the set  $L(0)$  will be considered as input, which will only contain the three original vertices of the corresponding sensor’s FoV.

The defined steps are derived and extended from our previous work in [29], resulting in more comprehensive and robust processing steps, described as follows:

- **Step 1:** The *intersection* vertices. These vertices are resulted from the intersection of an obstacle's line and one line of the considered FoV or OFoV. For any two different points  $(x_1, y_1)$  and  $(x_2, y_2)$ , the linear equation to be considered will take the form  $(x_2 - x_1)(y - y_1) = (y_2 - y_1)(x - x_1)$ ;
- **Step 2:** The *inside* vertices. When one or two vertices of the considered obstacle are inside the FoV or OFoV, they will be included as a vertex of the computed OFoV. The verification if a point is inside the original FoV (triangle) is easy, but it gets tricky when a point is checked against an OFoV defined as a concave polygon, as discussed in next subsection;
- **Step 3:** Inclusion of vertex  $A$  of the original FoV. The vertex  $A$  is the sensor's position and thus it must be in any computed OFoV. Because of this characteristic, the vertex  $A$  will guide the ordering of the vertices in any computed set  $L$ ;
- **Step 4:** Selection of some vertices of the original FoV or OFoV. There are some vertices in  $L(i - 1)$  that will be replicated into  $L(i)$ . In this processing step, the line equation defined when taking vertex  $A$  and any "adjacent" vertex of the original FoV ( $B$  or  $C$  vertices) or of the considered OFoV must not intersect the processed line of an obstacle. If there is no intersection, the considered adjacent vertex is included into the set of occlusion vertices;
- **Step 5:** *Induced* vertices. They result from an intersection of the linear equation created by vertex  $A$  and by an *inside* vertex (from Step 2), with the line of the side of an original FoV or OFoV. In a simple analysis, the *induced* vertices are resulted from the "shadow" created by an obstacle, since part of the original FoV will not be viewed anymore;
- **Step 6:** Removal of internal *induced* vertices. The *induced* vertices are fundamental when computing the OFoV, but for  $i$  as the last iteration for a particular obstacle  $o$ , the set  $L(i)$  must not have an *induced* vertex if it is "blocked" by two lines. Actually, for any *inside* vertex, the same *induced* vertex will always be computed twice since that vertex will be part of two concurrent lines. However, in the second computation, internal (blocked) *induced* vertices must to be removed, as depicted in Fig. 3 (in "Sensor 2" there is no *induced* vertex resulted from the intersection of line  $\overline{A(2)V_3}$  and a line of the original FoV, but an *induced* vertex is in the final set  $L$  in "Sensor 5" since it is not "blocked").

Following all defined steps and after the last iteration, the final set  $L$  of occlusion vertices may be achieved for the visual sensor  $s$ , resulting in  $L_{(s)} = \{(V_{(1)}x, V_{(1)}y), (V_{(2)}x, V_{(2)}y), \dots, (V_{(N)}x, V_{(N)}y)\}$ , for  $N$  vertices in  $L_{(s)}$  and  $(V_{(1)}x, V_{(1)}y) = (Ax_{(s)}, Ay_{(s)})$ . As those vertices create a polygon, the viewed area can be computed

using the Shoelace formula, as defined in Eq. 9.

$$P = \sum_{i=2}^N (V_{(i-1)}x \cdot V_{(i)}y - V_{(i)}x \cdot V_{(i-1)}y)$$

$$OFoV_{(s)} = \frac{|P + (V_{(N)}x \cdot V_{(1)}y - V_{(1)}x \cdot V_{(N)}y)|}{2} \quad (9)$$

Although the defined processing steps can be used to compute the vertices of the final OFoV, there are some important issues that must to be also considered, impacting on the selection of the faultless visual sensor nodes. Such issues are summarized as follows:

- If there is no computed *intersection* vertex (Step 1) or *inside* vertex (Step 2) in iteration  $i$ , then  $L(i) = L(i - 1)$ . In other words, the first two steps will indicate if the remaining processing steps need to be considered for the current iteration;
- A special condition that needs proper processing to avoid inconsistencies is when the vertices of the FoV or OFoV are coinciding with vertices of the obstacles. In such case, if the coinciding points are the only computed *intersection* vertices, the current FoV/OFoV must be assumed as the computed OFoV in the considered iteration. Otherwise, the OFoV computation must to be performed as already defined;
- When the same visual sensor is viewing more than one obstacle, previously computed *inside* vertices (Step 2) must be replicated into new computed  $L$  sets.

Actually, all defined steps and processing remarks are sufficient to compute the occlusion vertices for each visual sensor. However, such computations require the correct ordering of the vertices in each  $L_{(s)}$  set, as discussed in next subsection.

### C. ORDERING THE VERTICES IN EACH OFOV

After computing all the occlusion vertices in each (intermediate)  $L$  set, the vertices must to be ordered to correctly represent the defined OFoV in each iteration. This is required since the area of the OFoV and the computing of new occlusion vertices in further iterations can only be performed if the OFoV is correctly defined. However, there are different possible ways to order the occlusion vertices, resulting in different polygons. Fig. 4 presents examples of different polygons resulted from different orders for the vertices.

The computation of the OFoV's area (Eq. 9) can only be performed if the vertices in the set  $L$  are in a clockwise or anti-clockwise order, which lead us to define the ordered list  $L'$  as the result of this ordering process. But since there are different possible polygons depending on the number of occlusion vertices, a new method had to be created to compute the correct (clockwise or anti-clockwise) order for the vertices. The defined method takes the Vertex  $A$  as the reference for ordering, since it is the sensor's position, computing the order of the remaining vertices based on their angular distance to vertex  $A$  and a group of heuristics.

The angular distances are computed through the arc tangent function taking vertex  $A$  and each of the vertices in

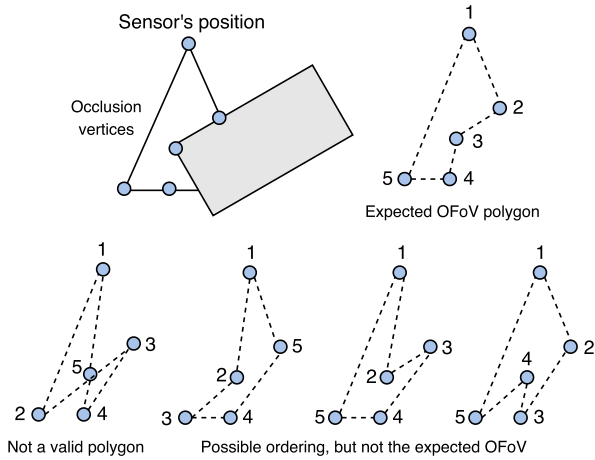


FIGURE 4. Ordering the list of occlusion vertices to create an OFoV.

the original set  $L$ , resulting in a numeric value ranging from  $-180^\circ$  to  $180^\circ$ . Each of the computed angles are assigned to the considered vertices, allowing the sorting of the vertices according to their angular distances to vertex  $A$ . However, as the angular distance of vertex  $A$  itself will be  $0^\circ$ , we sum  $180^\circ$  to all negatives vertices, resulting in a sorting scope from  $0^\circ$  to  $180^\circ$ .

When the computed angular distances are negative, the summing of  $180^\circ$  results in a quadrant shift of the considered vertex, assuming that the vertices will be in one of four different quadrants with vertex  $A$  at the center. In this case, if there is only one quadrant shift in an entire set  $L$ , the angular distance of vertex  $A$  is recomputed to  $90^\circ$ , keeping the expected “shape” for the OFoV. After that, any sorting algorithm can be employed (e.g. bubblesort), producing a list  $L'$  with the vertices in a clockwise or anti-clockwise order (depending on the employed sorting algorithm).

Although this process is expected to efficiently organize the vertices, a recurrent problem will be resulted from vertices with the same angular distance to vertex  $A$ . Actually, this may be particularly common, as depicted in Fig. 4: considering the correct ordering for the vertices, vertex 3 and vertex 4 have the same angular distance. In this case, any ordering algorithm will not differentiate those vertices, but there will be only one correct order when defining the OFoV. Therefore, we had to develop some heuristics to guide the correct ordering for the vertices.

Considering the expected formats for the OFoV, which is guided by the vertex  $A$  and the expected configurations of possible occlusions caused by rectangle-shaped obstacles, as expressed in Fig. 3, there will be some well-defined viewing limits for the visual sensors when they are occluded. Therefore, as an effective solution for the problem of vertices with the same angular distance, the proposed ordering algorithm will differentiate vertices from the original FoV triangle and vertices created by occlusion. Then, the “type” of the vertices will be considered along with a second decision parameter: the Euclidean distance of the considered vertex to vertex  $A$ . Doing so, after the initial ordering of the vertices

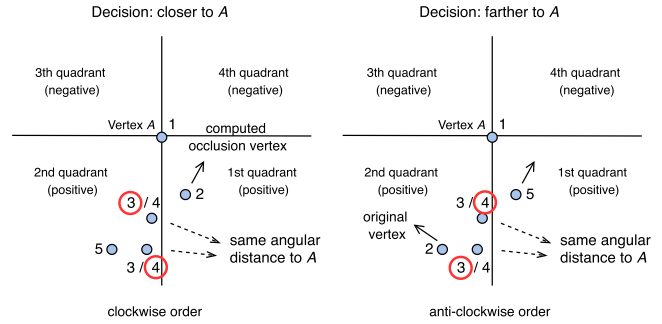


FIGURE 5. Applying the proposed heuristics for vertices with the same angular distance.

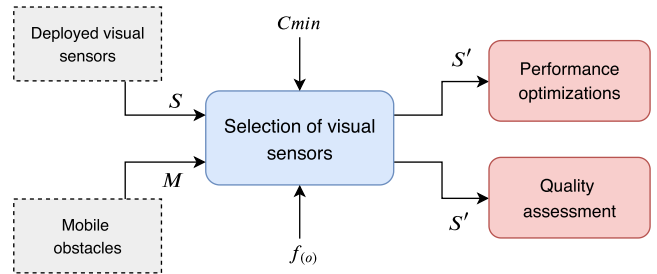


FIGURE 6. Proposed selection of faultless visual sensor nodes.

assuming only the angular distances as the single sorting parameter, a second round will process only vertices with the same angular distance, taking as reference the previous vertex in the computed order. For them, the Euclidean distance will be used as a second comparison parameter according to the following heuristic: the vertex with the highest distance must be “closer” to an original vertex of the FoV triangle, while the opposite applies for a vertex created by occlusion. Fig. 5 presents an example of this solution for both clockwise and anti-clockwise orders, taking as reference the occlusion configuration previously depicted in Fig. 4.

The ordering of the vertices must be performed for every iteration in a particular visual sensor, allowing the correct definition of intermediate OFoVs. Doing so, any number of non-coincident obstacles can be processed for a single visual sensor, resulting in the correct representation of the ultimately computed OFoV.

### V. SELECTING VISUAL SENSOR NODES

The proposed mathematical model is intended to allow the dynamic identification or even estimation (through simulation) of coverage failures, which are an important source of quality impairments in wireless visual sensor networks. Exploiting this model, it is possible to select only the visual sensors that should be considered when performing any kind of optimization or quality assessment in those networks, being a preprocessing step for many applications.

The selection of visual sensors will be performed based on the defined mathematical model and thus it should be executed in a central unit with proper knowledge of the entire network. Being performed mathematically, the sensors do not



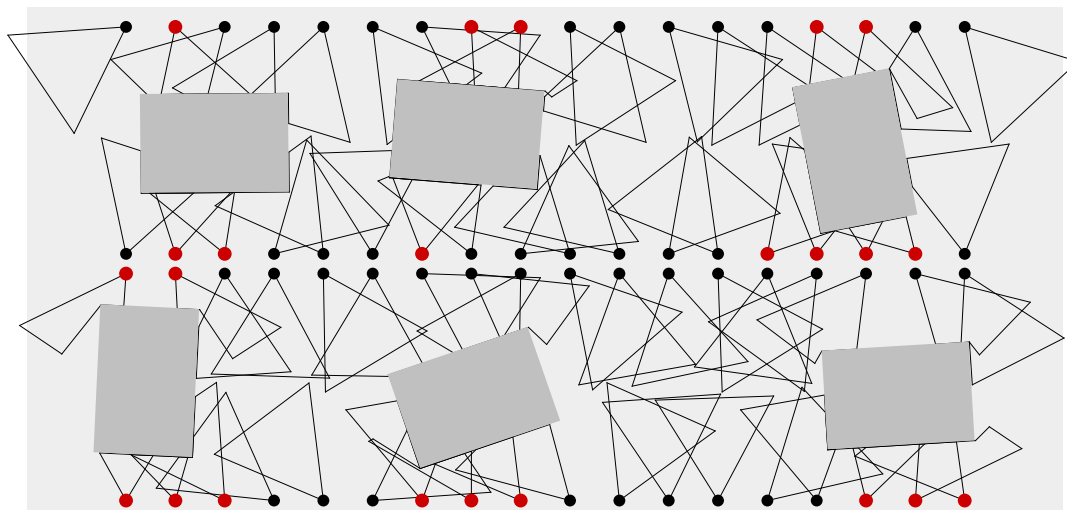


FIGURE 7. Selecting visual sensors for  $\theta_{(s)} = 60^\circ$ ,  $r_{(s)} = 120m$ ,  $Cmin = 0.6$  and  $t = 1$ .

get an additional processing burden having to compute the actual presence of obstacles. Otherwise, visual computing algorithms would be necessary to process visual data for occlusions, which might be a very costly task. Therefore, the proposed approach is intended to identify coverage failures in a simplified but still effective way.

The visual sensors selection mechanism will take as input the original set of visual sensors  $S$ , the current configuration of mobile obstacles  $M$  (that will change along the time) and the defined condition for coverage failure. This last parameter is established as the constant  $Cmin$ , which is considered when computing the relation between the original FoV and the computed OFoV. For  $0 \leq Cmin \leq 1.0$ , a coverage failure will occur when  $Cmin > (OFoV/FoV)$ .

Fig. 6 presents the overall procedure when selecting visual sensors. After taking all inputs and performing the expected mathematical computations, the set of selected (faultless) visual sensors,  $S'$ , can be informed to any requesting optimization or quality assessment mechanism. The selection of the visual sensors will be performed under the frequency  $f_{(o)}$ , which should be configured according to the characteristics of the considered system.

## VI. SIMULATIONS AND NUMERICAL RESULTS

The proposed mathematical model allows the dynamic identification of coverage failures, which may be exploited when selecting a group of visual sensors for any kind of optimization or quality assessment in visual sensor networks. Such selection will be performed without processing any visual data, achieving an approximated solution with reasonable computational cost and complexity. In order to demonstrate the use of the proposed approach in different scenarios, a group of simulations was performed. In first place, those simulations are intended to serve as an initial validation phase of the proposed solution, indicating that the model is correct. Actually, as the problem of visual occlusion caused by mobile

obstacles had not been addressed before, comparisons among different models would not achieve the expected outcome. Secondly, the presented results are valuable when associating different parameters of visual sensor nodes and obstacles, supporting analysis when selecting faultless visual sensors.

The entire model was implemented in Java/Python programming languages and simulated with different configuration parameters, strictly following the proposed rules and procedures. This implementation was composed of two modules: a) a Java-based tool to graphically exhibit the complete configuration of any scenario (visual sensors, obstacles and faulty nodes) and b) a module to save numerical results into ordinary files that are formatted by a Python script and processed by the Gnuplot open-source tool. Some results of both modules are presented and discussed in this section.

Initially, the visual tool was used to check the effectiveness of the proposed approach, for different configurations of sensors and obstacles. This phase of tests was intended to validate the proposed model and to easily identify implementation errors. After a consistent group of tests, assuming orientations for visual sensors from  $0^\circ$  to  $(180 - \theta_{(s)})^\circ$  and obstacles in different positions and with different dimensions, the results satisfactorily indicated that the proposed model is correct and that it can be used to select faultless sensors.

In order to better demonstrate the results of this phase, three different moments were selected to be displayed, for the same random configuration of visual sensors' orientations, and assuming  $\theta = 60^\circ$  and  $r = 120m$  for all deployed 72 visual sensors. In this scenario, visual sensors are covering two movement "tracks" for the mobile obstacles, with each track being 1000m long and 250m broad. Moreover, each track comprises 36 visual sensors (18 sensors in each side) for neighboring nodes with a distance of 50m between them.

For obstacles with  $w_{(o)} = 150m$  and height  $h_{(o)} = 100m$ , moving from the left to the right without intersecting each other, three different moments are presented in Fig. 7, Fig. 8

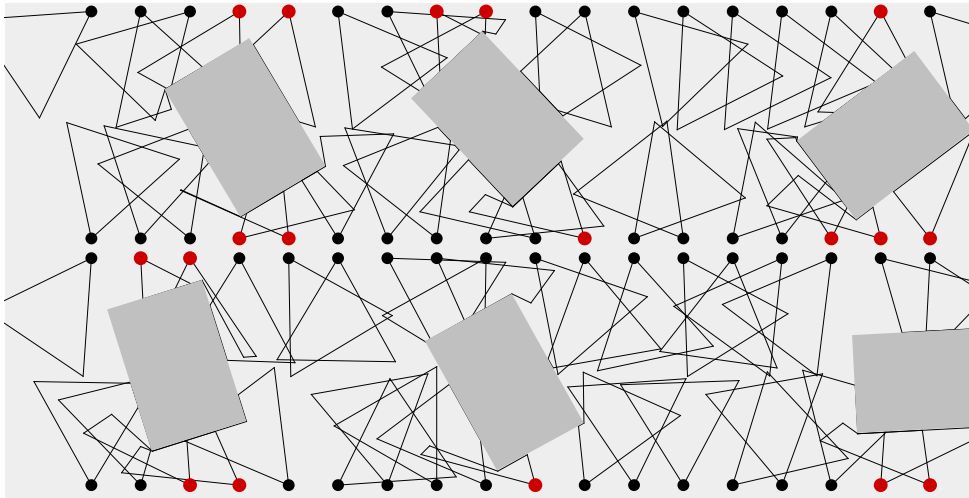


FIGURE 8. Selecting visual sensors for  $\theta_{(s)} = 60^\circ$ ,  $r_{(s)} = 120m$ ,  $Cmin = 0.6$  and  $t = 2$ .

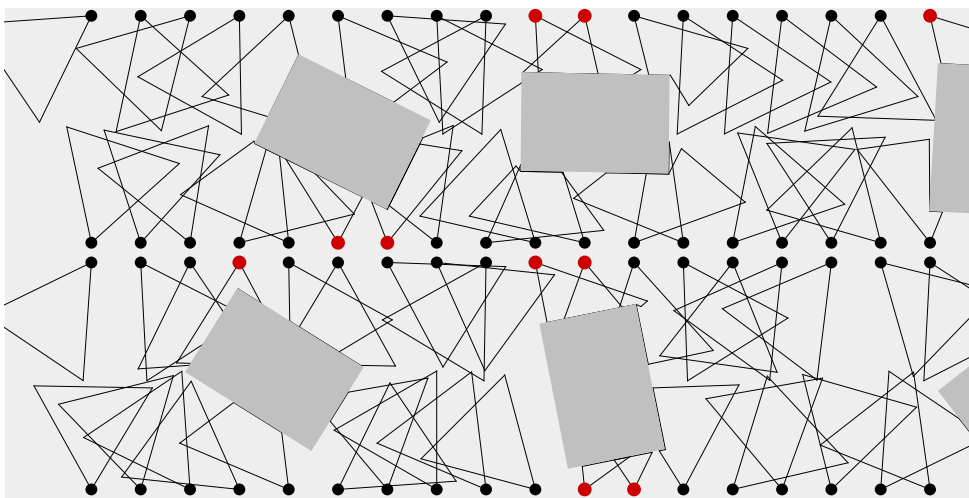


FIGURE 9. Selecting visual sensors for  $\theta_{(s)} = 60^\circ$ ,  $r_{(s)} = 120m$ ,  $Cmin = 0.6$  and  $t = 3$ .

and Fig. 9, assuming  $Cmin = 0.6$  (the visual sensors marked in red are faulty and they will not be selected).

It is interesting to note the impact of the mobile obstacles while they move over the considered monitored field. Depending on the configuration of the elements, different OFoV can be computed for each occluded sensor, directly impacting on the selection of visual sensors.

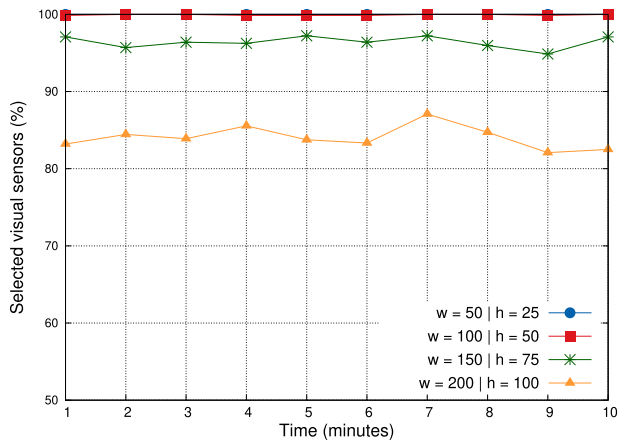
The second round of simulations tested different configurations of obstacles and visual sensors, systematically, highlighting the dynamics of the process of visual sensors selection. For that, it was considered subsequent moments with the same time interval, defined in minutes. The idea is that such tests could be valuable when planning a network for an expected deployment scenario.

Fig. 10 presents the percentage of selected visual sensors for 6 obstacles with different dimensions, for the same scenario with 72 visual sensors with  $\theta_{(s)} = 60^\circ$  and  $r_{(s)} = 120m$ ,

and for  $Cmin = 0.4$ . The presented results took 10 different sample times (in minutes), considering a slow movement of the obstacles over the track defined by the visual sensors, from the left to the right. After 10 minutes, the obstacles moved 300m with random orientations (they can freely rotate) and in a constant speed (30m/minute). Moreover, as the orientations of the visual sensors are randomly defined, within a range from  $0^\circ$  to  $180^\circ$  (keeping them covering the defined “track”), the presented results in Fig. 10 are average results after 10 consecutive tests.

In order to assess the impact on the percentage of selected visual sensors for a more restrictive condition of coverage failure, Fig. 11 presents results for  $Cmin = 0.8$  and the same configurations of the previous test.

Actually, both Fig. 10 and Fig. 11 present the percentage of selected visual sensors for 4 different configurations (width and height) of 6 mobile obstacles. However, for  $Cmin = 0.4$ ,



**FIGURE 10.** Percentage of selected visual sensors for  $\theta_{(s)} = 60^\circ$ ,  $r_{(s)} = 120m$  and  $Cmin = 0.4$ .

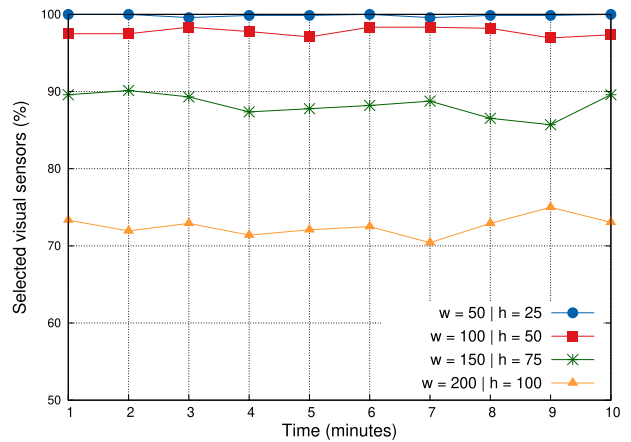


**FIGURE 12.** Percentage of selected visual sensors for  $\theta_{(s)} = 60^\circ$ ,  $r_{(s)} = 200m$  and  $Cmin = 0.4$ .

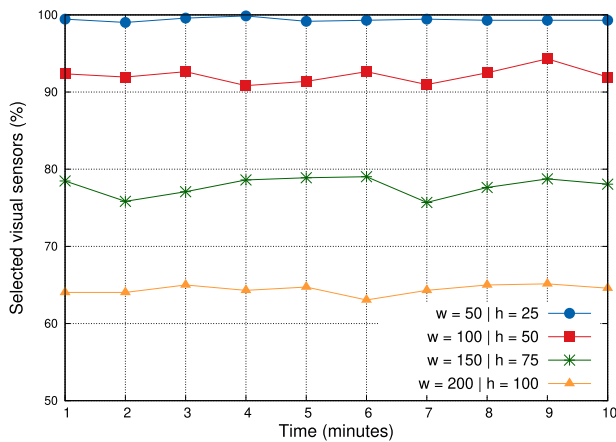


**FIGURE 11.** Percentage of selected visual sensors for  $\theta_{(s)} = 60^\circ$ ,  $r_{(s)} = 120m$  and  $Cmin = 0.8$ .

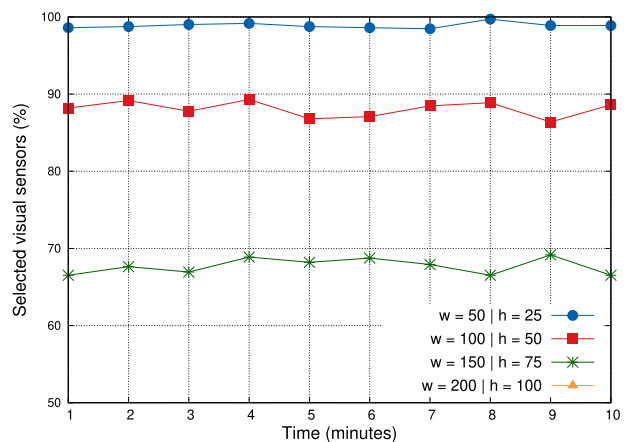


**FIGURE 13.** Percentage of selected visual sensors for  $\theta_{(s)} = 60^\circ$ ,  $r_{(s)} = 120m$  and  $Cmin = 0.8$ , for 8 obstacles. The percentage of selected sensors for  $w = 200 | h = 100$  was under 50% in all considered instants of time.

a computed OFoV will be assumed as valid when it has an area of at least 40% of the original FoV, which can be roughly considered as a “soft” condition for definition of a coverage failure in many scenarios. As a result, the percentage of selected visual sensors in Fig. 10 is not severely reduced, specially for small obstacles. On the other hand, higher values of  $Cmin$  will increase the probability of coverage failures in a visual sensor network, reducing the percentage of faultless visual sensor nodes, as depicted in Fig. 11.

The impact of occlusion on visual sensors with higher FoV areas was also assessed. Fig. 12 presents results for visual sensors with a higher sensing radius and  $Cmin = 0.4$ .

Fig. 10 and Fig. 12 present results for the same value of  $Cmin$ , but considering different sensing radius of the visual sensors. In the case of Fig. 12, a higher FoV area in the considered scenario increased the area occluded by the obstacles, which also increased the average number of faulty sensors, although the total viewed (and occluded) area may be higher.

Finally, the impact of occlusion caused by more obstacles was also assessed. The results in Fig. 13 shows the percentage of selected visual sensors for 8 mobile obstacles, with

4 obstacles in each of the moving tracks. The results can then be compared to Fig. 11, since all other parameters are the same. As can be seen in Fig. 13, more obstacles resulted in more occlusions, reducing the percentage of selected visual sensors.

In all performed experiments, the value of  $Cmin$  indirectly determined what must be assumed as a coverage failure, but the actual number of selected visual sensors will depend on other factors that should be properly considered. As mentioned before, it is expected that the establishment of  $Cmin$  will be a function of the monitoring requirements of each considered application. Therefore, knowing the “resistance” of the considered visual sensor network to occlusions ( $Cmin$  constant), the configurations of the sensors and the obstacles that will be passing by, visual sensing applications can be more efficiently designed.

The performed mathematical simulations presented some results concerning the impact of mobile obstacles in different scenarios. These results are initial indications that the proposed mathematical model can be used for analyses of visual

sensors configurations and deployments in the presence of mobile obstacles, with promising contributions to the area.

## VII. RESEARCH ISSUES WHEN SELECTING VISUAL SENSOR NODES

The adoption of visual sensing as an effective way to retrieve relevant data in a large set of innovative applications has opened many opportunities for monitoring in different contexts. Using cameras, sensors can gather still images or video streams from defined areas, and such scope can be even enlarged when specialized cameras are employed, as the ones with infrared or ultraviolet sensing capabilities. This resulted landscape of visual monitoring services supported by distributed self-organized sensor networks has found its place in many scenarios, as in industrial control, disaster detection, traffic management, public security, among many others.

There have been much research and development efforts around the so-called wireless visual sensor networks, with different approaches striving to soften the processing and transmission burden of visual data sensing. On a parallel research trend, quality assessment has been often desired in many contexts, with different approaches exploiting different quality perspectives. In all these cases, visual sensors have played a central role, guiding optimization strategies and quality assessment solutions.

When wondering about the next research steps in visual sensor networks, some directions can be highlighted, discussed as follows:

- **Availability:** this is a major concern, specially in critical applications as in industrial monitoring and control tasks. In short words, availability is related to the way an expected service will be provided, even in the occurrence of some failure. This goal has been pursued assessing, preventing and correcting major hardware and communication failures. Actually, due to the inherent risks of critical applications, availability should be considered as a central design issue and the same is true when visual sensors are employed. Therefore, as discussed in this article, availability should be considered along with the presence of coverage failures, which demand a proper visual sensors selection mechanism;
- **Networking:** wireless sensor networks have particular networking problems and the addition of sources of visual data potentially increases the communications complexities. Some approaches have already differentiated visual sensors from regular scalar sensors, reconfiguring the way transmissions are performed. Once again, such approaches should consider the existence of coverage failures and the possibility to apply some unified visual sensors selection approach;
- **Security:** traditionally, security has been put aside due to the resource constrained nature of sensor networks. However, visual sensing may impose some confidentiality demands, which may impact the overall quality of the network. In such cases, coverage failures should be

considered when allocating and authorizing the use of networks resources;

- **Visual localization and tracking:** many problems related to localization and tracking of targets have been proposed in the last years, exploiting the power of visual data processing. The use of mobile and rotatable cameras has also enhanced the applicability of WWSN. Nevertheless, a proper selection of visual sensors should be performed, removing visual sensors that are experiencing some kind of coverage failure.

In all presented research scenarios, a group of visual sensors will be considered for quality assessment or optimization for quality enhancement, or even both. However, we argue that such group of visual sensors may be not accurate due to visual coverage failures, as discussed in this article. In fact, there may be different causes for coverage failures and additional research is still required to find and to model each of such causes. In this sense, besides occlusion caused by mobile obstacles, we expect at least the following causes for coverage failures:

- **Light exposition:** when regular cameras are employed, the ambient light may determine if a certain visual sensor is under a coverage failure, since the retrieved visual data may become useless under low ambient light. For outdoor monitoring, visual sensors may also become faulty during the night;
- **Dust or heavy rain:** visual data processing algorithms may be used to identify if a camera's lens is dirty or with too many water drops. Alternatively, additional sensors may identify adverse weather conditions that can be mathematically computed when processing coverage failures;
- **Undesired orientation:** if visual sensors are viewing areas that are not intended by a particular application, they may be assumed as faulty nodes, even though their FoV are not occluded.

Coverage failures may be also processed as being a total or partial situation, depending on the application monitoring requirements. This perception may result in visual sensors being processed with some level of priority, weighting the operation of the network.

Finally, it is expected that the adoption of faultless visual sensors selection as a preprocessing mechanism can bring significant results for optimization and quality assessment in (wireless) visual sensor networks.

## VIII. CONCLUSION

The use of visual sensors for monitoring functions has become common due to the advent of low-cost and efficient camera-enabled sensor devices. This trend has put "visual sensing" as a common issue when proposing optimization and quality assessment approaches in wireless sensor networks. However, the processing of visual sensing without the proper understanding of coverage failures may result in imprecise results. The modelling of mobile obstacles is then

an initial step for more comprehensive handling of visual sensing.

This article presented a mathematical model to process dynamic occlusion and showed some initial results when associating different configuration parameters of visual sensors and mobile obstacles. Moreover, the concept of minimum expected coverage was also defined, which is the key element of the proposed visual sensors selection mechanism.

As future works, mobile obstacles will be modelled in a more precise way, considering groups of polygons when defining them. Additional results will also be sought, assuming more complex scenarios. Finally, the proposed mathematical model will be validated comparing to computer vision algorithms, assessing the precision of the simulated results.

## REFERENCES

- [1] F. Karray, M. W. Jmal, A. Garcia-Ortiz, M. Abid, and A. M. Obeid, "A comprehensive survey on wireless sensor node hardware platforms," *Comput. Netw.*, vol. 144, pp. 89–110, Oct. 2018.
- [2] D. Costa and C. Duran-Faundez, "Open-source electronics platforms as enabling technologies for smart cities: Recent developments and perspectives," *Electronics*, vol. 7, no. 12, p. 404, Dec. 2018.
- [3] J. Lin, W. Yu, N. Zhang, X. Yang, H. Zhang, and W. Zhao, "A survey on Internet of Things: Architecture, enabling technologies, security and privacy, and applications," *IEEE Internet Things J.*, vol. 4, no. 5, pp. 1125–1142, Oct. 2017.
- [4] C. Perera, C. H. Liu, and S. Jayawardena, "The emerging Internet of Things marketplace from an industrial perspective: A survey," *IEEE Trans. Emerg. Topics Comput.*, vol. 3, no. 4, pp. 585–598, Dec. 2015.
- [5] A. Gharaibeh, M. A. Salahuddin, S. J. Hussini, A. Khreishah, I. Khalil, M. Guizani, and A. Al-Fuqaha, "Smart cities: A survey on data management, security, and enabling technologies," *IEEE Commun. Surveys Tuts.*, vol. 19, no. 4, pp. 2456–2501, 4th Quart., 2017.
- [6] J. Nilsson and F. Sandin, "Semantic interoperability in industry 4.0: Survey of recent developments and outlook," in *Proc. IEEE 16th Int. Conf. Ind. Informat. (INDIN)*, Jul. 2018, pp. 127–132.
- [7] R. Kamath, M. Balachandra, and S. Prabhu, "Raspberry pi as visual sensor nodes in precision agriculture: A study," *IEEE Access*, vol. 7, pp. 45110–45122, 2019.
- [8] M. Irfan, L. Marcenaro, and L. Tokarchuk, "Crowd analysis using visual and non-visual sensors, a survey," in *Proc. IEEE Global Conf. Signal Inf. Process. (GlobalSIP)*, Dec. 2016, pp. 1249–1254.
- [9] H. Zannat, T. Akter, M. Tasnim, and A. Rahman, "The coverage problem in visual sensor networks: A target oriented approach," *J. Netw. Comput. Appl.*, vol. 75, pp. 1–15, Nov. 2016.
- [10] Y. Wang, S. Wu, Z. Chen, X. Gao, and G. Chen, "Coverage problem with uncertain properties in wireless sensor networks: A survey," *Comput. Netw.*, vol. 123, pp. 200–232, Aug. 2017.
- [11] P. Spachos and D. Hatzinakos, "Data relevance dynamic routing protocol for wireless visual sensor networks," in *Proc. 18th Int. Conf. Digit. Signal Process. (DSP)*, Jul. 2013, pp. 1–6.
- [12] H. R. Al-Zoubi, "Video coding and routing in wireless video sensor networks," *AASRI Procedia*, vol. 5, pp. 48–53, Jan. 2013.
- [13] C. Duran-Faundez, D. G. Costa, V. Lecuire, and F. Vasques, "A geometrical approach to compute source prioritization based on target viewing in wireless visual sensor networks," in *Proc. IEEE World Conf. Factory Commun. Syst. (WFCS)*, May 2016, pp. 1–7.
- [14] T. Jesus, P. Portugal, F. Vasques, and D. Costa, "Automated methodology for dependability evaluation of wireless visual sensor networks," *Sensors*, vol. 18, no. 8, p. 2629, Aug. 2018.
- [15] V. P. Munishwar and N. B. Abu-Ghazaleh, "Coverage algorithms for visual sensor networks," *ACM Trans. Sensor Netw.*, vol. 9, no. 4, pp. 1–36, Jul. 2013.
- [16] E. O. Rangel, D. G. Costa, and A. Loula, "On redundant coverage maximization in wireless visual sensor networks: Evolutionary algorithms for multi-objective optimization," *Appl. Soft Comput.*, vol. 82, Sep. 2019, Art. no. 105578.
- [17] R. Ghazalian, A. Aghagolzadeh, and S. M. H. Andargoli, "Wireless visual sensor networks energy optimization with maintaining image quality," *IEEE Sensors J.*, vol. 17, no. 13, pp. 4056–4066, Jul. 2017.
- [18] D. Costa, L. Guedes, F. Vasques, and P. Portugal, "Research trends in wireless visual sensor networks when exploiting prioritization," *Sensors*, vol. 15, no. 1, pp. 1760–1784, Jan. 2015.
- [19] V. Bhandary, A. Malik, and S. Kumar, "Routing in wireless multimedia sensor networks: A survey of existing protocols and open research issues," *J. Eng.*, vol. 2016, Apr. 2016, Art. no. 9608757.
- [20] P. Xu, I.-H. Chang, C.-Y. Chang, B. Dande, and C.-Y. Hsiao, "A distributed barrier coverage mechanism for supporting full view in wireless visual sensor networks," *IEEE Access*, vol. 7, pp. 156895–156906, 2019.
- [21] D. Costa, I. Silva, L. Guedes, F. Vasques, and P. Portugal, "Availability issues in wireless visual sensor networks," *Sensors*, vol. 14, no. 2, pp. 2795–2821, Feb. 2014.
- [22] B. Shahrokhzadeh and M. Dehghan, "A distributed game-theoretic approach for target coverage in visual sensor networks," *IEEE Sensors J.*, vol. 17, no. 22, pp. 7542–7552, Nov. 2017.
- [23] C.-F. Cheng and K.-T. Tsai, "Distributed barrier coverage in wireless visual sensor networks with  $\beta$ -QoM," *IEEE Sensors J.*, vol. 12, no. 6, pp. 1726–1735, Jun. 2012.
- [24] D. G. Costa, L. A. Guedes, F. Vasques, and P. Portugal, "QoV: Assessing the monitoring quality in visual sensor networks," in *Proc. IEEE 8th Int. Conf. Wireless Mobile Comput., Netw. Commun. (WiMob)*, Oct. 2012, pp. 667–674.
- [25] K. R. Konda, N. Conci, and F. De Natale, "Global coverage maximization in PTZ-camera networks based on visual quality assessment," *IEEE Sensors J.*, vol. 16, no. 16, pp. 6317–6332, Aug. 2016.
- [26] F. Yap and H.-H. Yen, "A survey on sensor coverage and visual data capturing/processing/transmission in wireless visual sensor networks," *Sensors*, vol. 14, no. 2, pp. 3506–3527, Feb. 2014.
- [27] D. G. Costa, I. Silva, L. A. Guedes, P. Portugal, and F. Vasques, "Selecting redundant nodes when addressing availability in wireless visual sensor networks," in *Proc. 12th IEEE Int. Conf. Ind. Informat. (INDIN)*, Jul. 2014, pp. 130–135.
- [28] M. Alaei and J. M. Barcelo-Ordinas, "Node clustering based on overlapping FoVs for wireless multimedia sensor networks," in *Proc. IEEE Wireless Commun. Netw. Conf.*, Sydney, NSW, Australia, Apr. 2010, pp. 1–6.
- [29] D. G. Costa, F. Vasques, and P. Portugal, "Enhancing the availability of wireless visual sensor networks: Selecting redundant nodes in networks with occlusion," *Appl. Math. Model.*, vol. 42, pp. 223–243, Feb. 2017.
- [30] D. G. Costa and C. Duran-Faundez, "Assessing availability in wireless visual sensor networks based on Targets' perimeters coverage," *J. Electr. Comput. Eng.*, vol. 2016, pp. 1–14, Oct. 2016.
- [31] F. G. H. Yap and H.-H. Yen, "Novel visual sensor deployment algorithm in occluded wireless visual sensor networks," *IEEE Syst. J.*, vol. 11, no. 4, pp. 2512–2523, Dec. 2017.
- [32] K. Scott, R. Dai, and M. Kumar, "Occlusion-aware coverage for efficient visual sensing in unmanned aerial vehicle networks," in *Proc. IEEE Global Commun. Conf. (GLOBECOM)*, Dec. 2016, pp. 1–6.
- [33] L. Anuj and M. T. G. Krishna, "Multiple camera based multiple object tracking under occlusion: A survey," in *Proc. Int. Conf. Innov. Mech. for Ind. Appl. (ICIMIA)*, Feb. 2017, pp. 432–437.
- [34] A. Al-Kaff, D. Martín, F. García, A. D. L. Escalera, and J. María Armingol, "Survey of computer vision algorithms and applications for unmanned aerial vehicles," *Expert Syst. Appl.*, vol. 92, pp. 447–463, Feb. 2018.



**THIAGO C. JESUS** received the B.Sc. degree in computer engineering from the State University of Feira de Santana, Brazil, in 2008, the M.Sc. degree in electrical engineering from the Federal University of Rio de Janeiro, Brazil, in 2011, and the Ph.D. degree in electrical and computer engineering program at the Faculty of Engineering, University of Porto, Portugal. He is currently an Auxiliary Professor with the Department of Technology, State University of Feira de Santana, Brazil.

His research interests include dependability evaluation on wireless sensor networks, fault diagnosis of discrete event systems, industrial communication systems, and smart cities. In those areas, he acted as a reviewer for high-quality journals and is the author or coauthor of several articles.



**DANIEL G. COSTA** (Senior Member, IEEE) received the A.B.Sc. degree in computer engineering and the M.Sc. degree in electrical engineering from the Federal University of Rio Grande do Norte, in 2005 and 2006, respectively, and the D.Sc. degree in electrical engineering from the Federal University of Rio Grande do Norte, Brazil, in 2013, with research internship at the University of Porto, Portugal. He is currently an Associate Professor with the Department of Technology, State University of Feira de Santana, Brazil, where he also coordinates the Advanced Networks and Applications Lab, LARA. He has served several committees of distinguished international conferences and acted as reviewer for high-quality journals. He is the author or coauthor of more than 100 articles in the areas of computer networks, industrial communication systems, the Internet of Things, smart cities, and sensor networks.



**FRANCISCO VASQUES** received the Ph.D. degree in computer science from LAAS-CNRS, Toulouse, France, in 1996.

He has been an Associate Professor with the University of Porto, Portugal, since 2004. He is author or coauthor of more than 150 articles in the areas of real-time systems and industrial communication systems. His current research interests include real-time communication, industrial communication, and real-time embedded systems.

He is also a member of the Editorial Board of Sensors, MDPI, for the Sensor Networks Section, since 2018, and the *International Journal of Distributed Sensor Networks* (Hindawi). He is currently an Associate Editor of the IEEE Transactions on Industrial Informatics for the topic Industrial Communications, since 2007.



**PAULO PORTUGAL** received the Ph.D. degree in electrical and computer engineering from the Faculdade de Engenharia da Universidade do Porto (FEUP-UP), Porto, Portugal, in 2005. He is currently an Associate Professor with the Electrical and Computer Engineering Department (DEEC), FEUP-UP. His current scientific interests include industrial communications and dependability/performance modeling.



**ANA AGUIAR** graduated in electrical and computer engineering from the University of Porto, Porto, Portugal, and the Ph.D. degree in telecommunication networks from the Technical University of Berlin, Berlin, Germany. She is currently an Assistant Professor at FEUP and a Coordinator of the Instituto de Telecomunicações, Porto. Her research interests include in the field of wireless systems, specifically vehicular networks, the Internet of Things, and spatio-temporal data science.

She has collaborated in several interdisciplinary projects on smart cities and well-being. She co-founded a start-up on the protection of vulnerable road users, and she contributes as a reviewer or an organizing member to several IEEE and ACM conferences and journals.

...